sensors

Article

Super-Wide Impedance Bandwidth Planar Antenna for Microwave and Millimetre-Wave Applications

Mohammad Alibakhshikenari[1]*, Bal S. Virdee[2], Chan H. See[3,4], Raed A. Abd-Alhameed[5], Francisco Falcone[6], and Ernesto Limiti[1]

[1] Electronic Engineering Depart., University of Rome "Tor Vergata", Via del Politecnico 1, 00133 Roma, Italy
[2] London Metropolitan University, Center for Communications Technology, London N7 8DB, UK
[3] School of Eng. & the Built Environment, Edinburgh Napier University, 10 Colinton Rd., Edinburgh, EH10 5DT, UK
[4] School of Engineering, University of Bolton, Deane Road, Bolton, BL3 5AB, UK
[5] Faculty of Engineering & Informatics, University of Bradford, Bradford, West Yorkshire, BD7 1DP, UK
[6] Electric and Electronic Engineering Department, Universidad Pública de Navarra, SPAIN

* Correspondence: alibakhshikenari@ing.uniroma2.it

Abstract: The feasibility study of a novel configuration for a super-wide impedance planar antenna is presented based on a 2×2 microstrip patch antenna (MPA) using CST Microwave Studio. The antenna comprises a symmetrical arrangement of four-square patches that are interconnected to each other with cross-shaped high impedance microstrip lines. The antenna array is exciting through a single feedline connected to one of the patches. The proposed antenna array configuration overcomes the main drawback of conventional MPA of narrow bandwidth that is typically < 5%. The antenna exhibits a super-wide frequency bandwidth from 20 GHz to 120 GHz for S11<-15dB, which corresponds to a fractional bandwidth of 142.85%. The antenna's performance of bandwidth, impedance match, and radiation gain were enhanced by etching slots on the patches. With the inclusion of the slot the maximum radiation gain and efficiency of the MPA have increased to 15.11 dBi and 85.79% at 80 GHz, which show an improvement of 2.58 dBi and 12.54%, respectively. The dimension of each patch antenna is 4.3×5.3 mm^2. The results show that the proposed MPA is useful for various communications existing and emerging systems such as ultra-wideband (UWB) communications, RFID systems, massive multiple-output multiple-input (MIMO) for 5G, and radar systems.

Keywords: Array antenna, Microstrip Patch Antenna (MPA), Slot Antenna, Simplified composite right/left-handed metamaterial (SCRLH MTM), Multiple-Output Multiple-Input (MIMO), Radar, radio frequency identification (RFID) systems, Millimetre-wave band

1. Introduction

Demand for antennas that possess desirable characteristics such as light weight, low profile and high gain have burgeoned significantly with the rapid development of modern wireless communication systems [1, 2]. Antennas implemented on microstrip medium exhibit some of these desirable properties which makes them very popular in RF/microwave transceiver systems as they are compatible with integrated circuit technology and are relatively cheap and easy to fabricate [3-10]. In addition, microstrip patch antennas (MPAs) can be made to be conformal to planar and non-planar surfaces. The radiation mechanism arises from discontinuities at each truncated edge of the microstrip transmission line. The radiation at the edges causes the antenna to act slightly larger electrically than its physical dimensions, so in order for the antenna to be resonant, a length of microstrip transmission line slightly shorter than one-half a wavelength at the frequency is used. Various techniques have been developed previously to enhance the antenna's impedance bandwidth and reduce its physical footprint, and hence the MPA has become extensively used in various wireless communication applications. Nevertheless, conventional microstrip patch antennas still suffer from narrow impedance bandwidth which is typically less than 5% and low radiation efficiency [1-4]. In addition, the operation of MPA is restricted to the microwave band.

In this paper, we have proposed a simple method to overcome the main drawback of the conventional microstrip patch antenna, and thereby realised a super-wide impedance bandwidth antenna. The design of the antenna is based on implementing four interconnected square patches in close proximity and arranged in an array configuration. Each patch constituting the antenna is loaded with the rectangular slot to improve its performances without increasing the size of the patches. This is implemented by simply etching a slot inside each radiating patch. The slot essentially like series left-handed capacitance and the resulting patch exhibits simplified composite right/left-handed (SCRLH) metamaterial properties [11-13]. The proposed microstrip patch antenna design is applicable for various communications existing and emerging systems such as ultra-wideband (UWB) communications, RFID systems, massive multiple-output multiple-input (MIMO) for 5G, and radar systems.

2. Proposed Microstrip Antenna Sructure

The proposed antenna structure is composed of four-square patches in a 2×2 arrangement, as shown in Fig. 1. The antennas are interconnected with a cross-shaped high-impedance line. The design of the square patches is based on conventional theory. The width and length of the patch were calculated using the following standard design equations [14].

$$Width = \frac{c}{2f_o\sqrt{\frac{\varepsilon_r+1}{2}}} \quad (1)$$

$$Length = \frac{c}{2f_o\sqrt{\varepsilon_{eff}}} - 0.824h\left[\frac{(\varepsilon_{eff}+0.3)\left(\frac{W}{h}+0.264\right)}{(\varepsilon_{eff}-0.258)\left(\frac{W}{h}+0.8\right)}\right] \quad (2)$$

$$\varepsilon_{eff} = \frac{\varepsilon_r+1}{2} + \frac{\varepsilon_r-1}{2}\left[\frac{1}{1+12\sqrt{\frac{h}{W}}}\right] \quad (3)$$

The microstrip patch was designed at 20 GHz on standard theory on a high frequency ceramic-filled PTFE composite dielectric substrate by Rogers RO3003 with dielectric constant of 3.0, loss-tangent of 0.001 and thickness of 0.13 mm. The physical dimensions of the proposed antenna configuration are given in Table I. The resulting antenna is low profile and simple to design and fabricate. Unlike conventional microstrip antenna arrays the proposed antenna array is excited through a single feedline connected to one of the antennas.

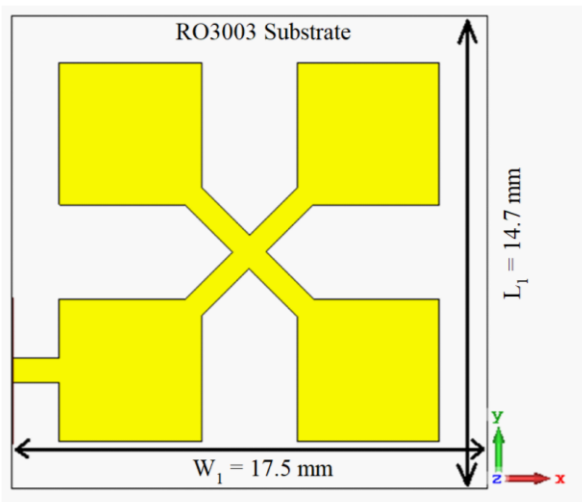

Figure 1. The proposed microstrip antenna array.

The reflection-coefficient response in Fig. 2 of the proposed MPA array structure shows its impedance bandwidth extends from 20 GHz to 120 GHz for S11 < -10 dB with four narrow band-notches at 62.5, 77.5, 97.5, and 120 GHz.

To improve the array's performances and extend its effective aperture area the four patches are loaded with a rectangular slot, as shown in Fig. 3. With the slots the reflection-coefficient is significantly improved. Now, the impedance bandwidth from 20 GHz to 120 GHz is achieved for S11 < -17.5 dB with no narrow band-notches. In the patch structure the slot essentially like series left-handed capacitance and the resulting patch exhibits simplified composite right/left-handed (SCRLH) metamaterial properties [11-13]. It is evident from Fig. 2 that there is a distinct improvement in the reflection-coefficient from 20-120 GHz. The improvement in the antenna's performance is attributed to a combination of metamaterial effects and the complex interaction resulting from the surface currents over the antenna and electromagnetic fields. With the proposed technique the dimensions of the antenna structure remain unaffected. It was however necessary to optimize the dimensions of the slots to enhance the reflection-coefficient response of the antenna array, and the optimised dimensions are given in Table 1.

The radiation gain and efficiency of the antenna array with no slot and with slot are shown in Figs. 4 and 5, respectively. These figures show with no slot the antenna gain and efficiency reach a peak of around 12.53 dBi and 73.25% at 80 GHz, respectively, however with application of slot the optimum gain and efficiency improve to 15.11 dBi and 85.79% at 80 GHz, respectively. Therefore, an average improvement of 2.58 dBi and 12.54% on the maximum radiation gain and efficiency have achieved, respectively. The details of the radiation properties have tabulated in Table 2.

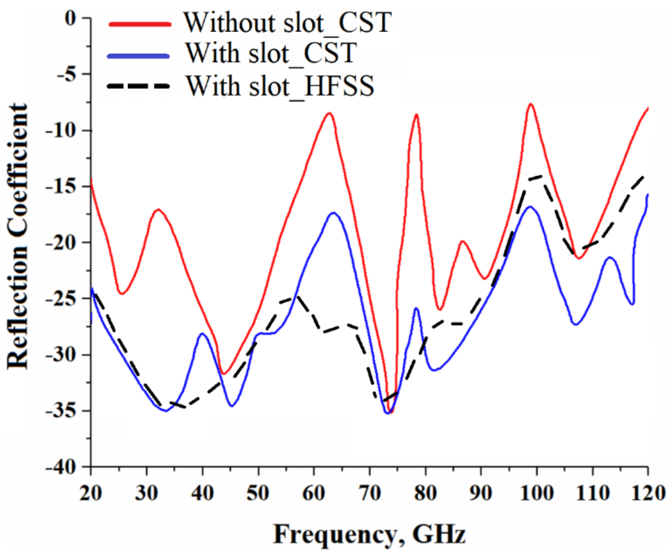

Figure 2. Reflection-coefficient (S_{11}<-10dB) response of the microstrip antenna array "without" slot and "with" slot using two different commercially available 3D full wave electromagnetics simulation tools (CST Microwave Studio® and HFSS™).

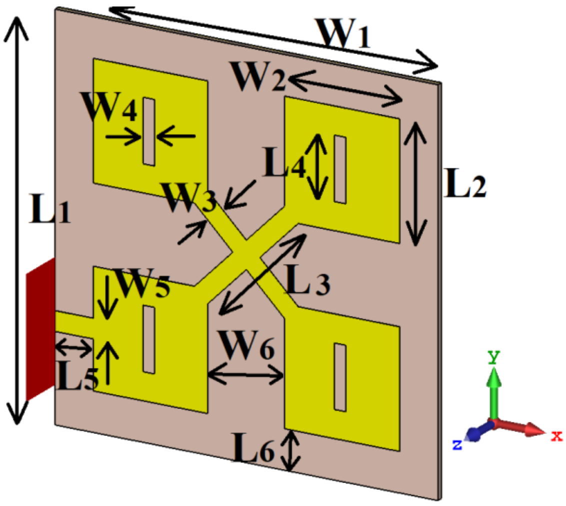

Figure 3. Configuration of the proposed microstrip antenna array with a ground-plane.

Table 1. Antenna Structural Parameters

L_1	14.7 mm	W_1	17.5 mm
L_2	4.3 mm	W_2	5.3 mm
L_3	4.5 mm ($\lambda_0/4$)	W_3	0.3 mm (50Ω)
L_4	4.3 mm (0.52×L_2)	W_4	0.52 mm (0.1×W_2)
L_5	2.4 mm ($\lambda_0/4$)	W_5	0.3 mm (50Ω)
L_6	2.4 mm ($\lambda_0/4$)	W_6	0.32 mm (0.6×W_2)

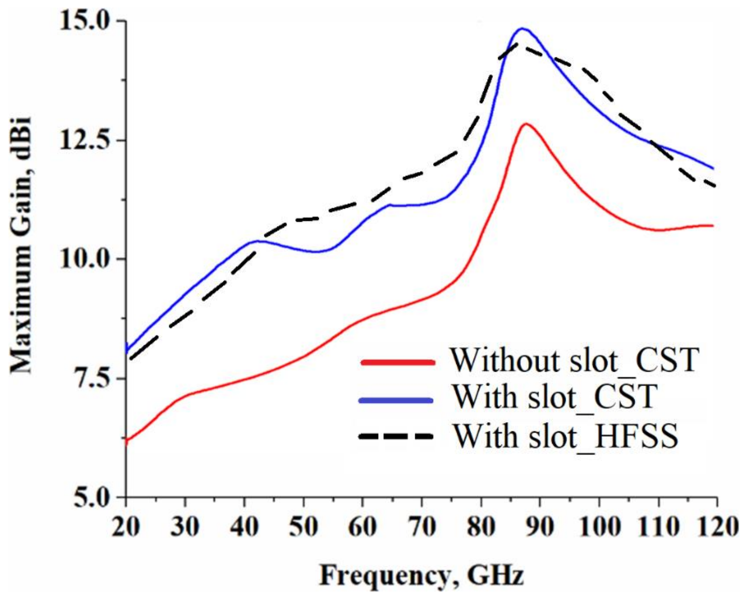

Figure 4. Gain response for both cases "with no" slot and "with" slot using two different commercially available 3D full wave electromagnetics simulation tools (CST Microwave Studio® and HFSS™).

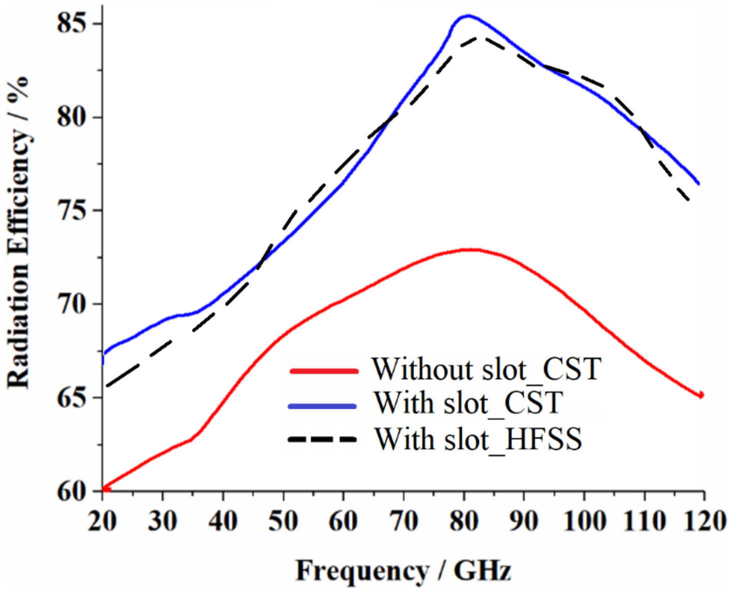

Figure 5. Radiation efficiency response for both cases "before apply" the slot and "after apply" the slot using two different commercially available 3D full wave electromagnetics simulation tools (CST Microwave Studio® and HFSS™).

Co- and cross (X) polarization radiation patterns of the proposed microstrip antenna array in the E- and H-planes are shown in Fig. 6 at spot frequencies of 30, 60, 90, and 120 GHz in its operating range. This show the antenna is directional in the E-plane with sidebands about 15 dB down from the main beam. It is observed that at 60 GHz the beamwidth doubles and the gain drops down by an average of 3 dB. In the H-plane the beamwidth extends from around -50 to +80 degrees and the radiation gain various with frequency. In both planes the cross polarization is significantly below the main beam.

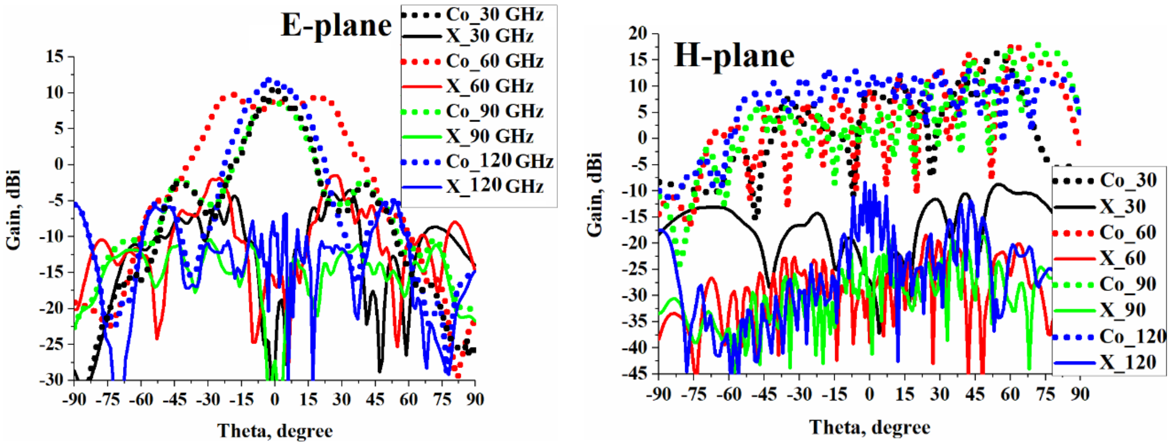

Figure 6. Co- and Cross-radiation patterns of the proposed microstrip antenna arrays "with" slots in the E- and H-planes at spot frequencies over its operating band.

The surface current distributions before and after applying the slots at an arbitrary frequency of 80 GHz in the antenna's operating range is shown in Fig. 7. This figure shows that with no slot the current is mainly concentrated around the excitation patch however when slots are introduced the current is more evenly distributed between the four patched. This reveals greater interaction is realized between the four patches that results in significantly improved reflection-coefficient over a super-wide frequency range.

Table 2. Radiation Performance Parameters.

Radiation gain (with no slot)		
Minimum	Maximum	Average
5.75 dBi	12.53 dBi	8 dBi
Radiation gain (with slot)		
7.88 dBi	15.11 dBi	12 dBi
Improvement		
2.13 dBi	2.58 dBi	4 dBi

Radiation efficiency (with no slot)		
Minimum	Maximum	Average
60.82%	73.25%	66%
Radiation efficiency (with slot)		
67.41%	85.79%	78%
Improvement		
6.95%	12.54%	12%

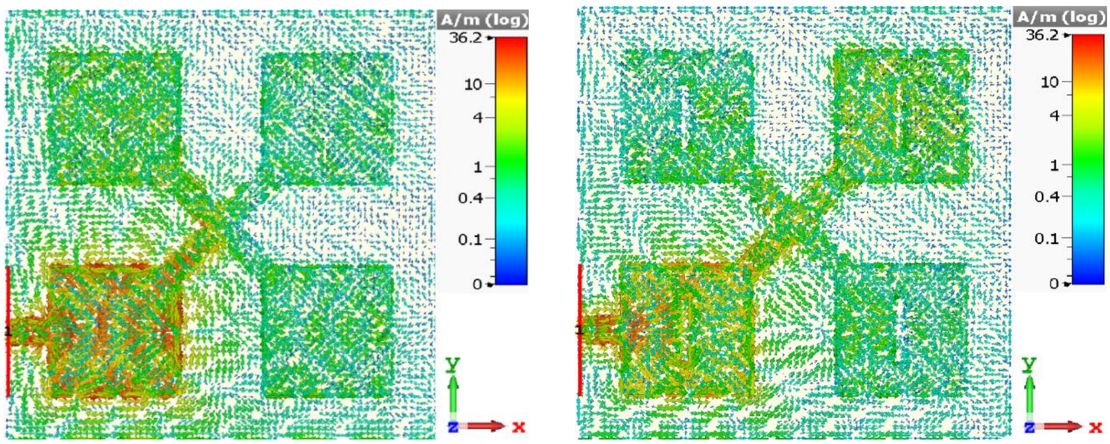

(a) “without” slots (b) “with” slots

Fig.7. Surface current distributions at spot frequency of 80 GHz, (a) “without” slots, and (b) “with” slots.

It is worth to comment that, to validate the results we have modelled and simulated the proposed structure with two different 3D full-wave electromagnetic simulation tools (CST Microwave Studio® and HFSS™). There is excellent correlation between CST Microwave Studio® and HFSS™ results. CST Microwave Studio® uses Method of Moments (MoM) to arrive at the solution whereas HFSS™ uses Finite Element Method (FEM).

3. Comparison with Other Recent Designs

The proposed antenna is compared planar wideband antennas reported to date design technique, size, dielectric constant and operating frequency. The comparison is summarized in Table 3. Compared to other antennas the proposed antenna has much smaller footprint and operates over significantly wider impedance bandwidth. In addition, it is simple to design and implement.

Table 3. Comparison with Recently Reported Antennas

Refs.	Technique	Antenna size (mm^3)	Dielectric constant	Operating frequency (GHz)
[16]	Inverted L-resonator	30.5 × 24 × 1.5	3.38	3.1–10.6
[17]	Annular slot	26 × 24 × 1.6	4.6	3–10.6
[18]	Rectangular slots	16 × 14 × 1	4.4	3.2–10
[19]	Circular slots	30 × 26 × 1.6	4.4	2.5–11
[20]	Inverted U-strip	50 × 45 × 1.27	6.0	3.1–10.6
[21]	Split ring resonators	30 × 26 × 1.6	3.5	2.4–10.1
[22]	lamp shaped antenna	28×15× 1.6	4.4	2.7–14
[23]	Cap. Integrated antenna	30.5 × 24 × 1.5	3.3	3.1–10.6
[24]	L-shaped stub	46 × 42 × 1	4.4	3.1–10.6
[25]	Loading quarter wavelength resonating strip	38 × 30 × 1.6	4.4	3.1–10.6 and 2.4–2.5
[26]	Loading TL-MTM within UWB antenna	38.5 × 46.4 × 1.6	4.4	3.1–10.6 and 2.43–2.49
[27]	No integration	52 × 32 × 1.6	4.4	3.1–10.6
[28]	Loading quarter wavelength resonating strip at the center of the patch	50 × 24 × 1.6	4.4	3.1–11.4 and 2.18–2.59
[29]	Loading parasitic strip	46 × 20 × 1.0	2.4	3.1–10.6 and 2.40–2.48
[30]	Loading quarter wavelength resonating strip at the center of the patch	42 × 24 × 1.6	4.4	3.1–12.0 and 2.30–2.50
[31]	Loading strip-line to the patch	45 × 32 × 1.0	4.4	3.1–10.6 and 2.40–2.50
[32]	Capacitors loaded miniaturized resonator in the ground plane	30 × 31 × 1.5	3.38	3.1–10.6 and 2.4–2.48
[33]	Band-pass filter integration	35 × 24.4 × 2	3.38	2.8–6
[34]	Dielectric loading	61 × 61 × 8	~4.0	1.6–12
This paper	**SCRLH metamaterial**	**4.3 × 5.3 × 0.13**	**3.0**	**20–120**

4. Conclusion

The feasibility of a novel configuration for a 2×2 microstrip patch antenna based on metamaterial concept using CST Microwave Studio is shown to exhibit super-wide impedance bandwidth extending from 20 GHz to 120 GHz for S11 <-15 dB, which corresponds to a fractional bandwidth of 142.85%. The average gain and radiation efficiency of the antenna are 12 dBi and 78%, respectively, which show 4.0 dBi and 12% improvement after applying the slots. The proposed antenna structure overcomes the narrow bandwidth of conventional microstrip patch designs. The antenna can be used at microwaves and millimetre-wave applications including UWB, RFID systems, massive MIMO for 5G, and radar systems.

Acknowledgments: This work was partially supported by innovation programme under grant agreement H2020-MSCA-ITN-2016 SECRET-722424 and the financial support from the UK Engineering and Physical Sciences Research Council (EPSRC) under grant EP/E022936/1.

References

1. D. M. Pozar, ''Microstrip antennas,'' Proc. IEEE, Vol. 80, No. 1, pp. 79–91, Jan. 1992.
2. K. F. Lee and K. M. Luk, Microstrip Patch Antennas. London, U.K.: Imperial College Press, 2011.
3. K. D. Xu, H. Xu, Y. Liu, J. Li, Q. H. Liu, "Microstrip Patch Antennas with Multiple Parasitic Patches and Shorting Vias for Bandwidth Enhancement," IEEE Access, Vol. 6, March 16, 2018, pp. 11624 – 11633.
4. K.-F. Lee, and K.-F. Tong, "Microstrip Patch Antennas-Basic Characteristics and Some Recent Advances", Proceedings of the IEEE, Vol. 100, No. 7, July 2012, pp. 2169-2180.
5. A. A. Deshmukh, ''Broadband slot cut shorted sectoral microstrip antennas,'' IET Microw., Antennas Propag., vol. 11, no. 9, pp. 1280–1287, Jul. 2017.
6. A. Kandwal and S. K. Khah, ''A novel design of gap-coupled sectoral patch antenna,'' IEEE Antennas Wireless Propag. Lett., vol. 12, pp. 674–677, 2013.
7. Z. Liang, J. Liu, Y. Zhang, and Y. Long, ''A novel microstrip quasi Yagi array antenna with annular sector directors,'' IEEE Trans. Antennas Propag., vol. 63, no. 10, pp. 4524–4529, Oct. 2015.
8. J. Wu, Y. Yin, Z. Wang, and R. Lian, ''Broadband circularly polarized patch antenna with parasitic strips,'' IEEE Antennas Wireless Propag. Lett., vol. 14, pp. 559–562, 2015.
9. J.-Y. Sze and K.-L. Wong, ''Slotted rectangular microstrip antenna for bandwidth enhancement,'' IEEE Trans. Antennas Propag., vol. 48, no. 8, pp. 1149–1152, Aug. 2000.
10. J.-H. Lu, ''Bandwidth enhancement design of single-layer slotted circular microstrip antennas,'' IEEE Trans. Antennas Propag., vol. 51, no. 5, pp. 1126–1129, May 2003.
11. M. Alibakhshi-Kenari, M. Naser-Moghadasi, R. A. Sadeghzadeh, B. S. Virdee, and E. Limiti, "New Compact Antenna Based on Simplified CRLH-TL for UWB Wireless Communication Systems," Int. Journal of RF and Microwave Computer-Aided Engineering, Vol. 26, Iss. 3, March 2016, pp. 217–225.
12. R. A. Sadeghzadeh, M. Alibakhshi-Kenari and M. Naser-Moghadasi, "UWB Antenna Based on SCRLH-TLs for Portable Wireless Devices," Microwave and Optical Technology Letters, Vol. 58, Iss. 1, January 2016, pp. 69–71.
13. M. Alibakhshikenari, M. Naser-Moghadasi, R. A. Sadeghzadeh, B. S. Virdee and E. Limiti, "New CRLH-Based Planar Slotted Antennas with Helical Inductors for Wireless Communication Systems, RF-Circuits and Microwave Devices at UHF-SHF Bands," Wireless Personal Communications, Springer Journal, Wireless Personal Communications, Feb. 2017, Vol. 92, Iss. 3, pp 1029–1038.
14. Microstrip Patch Antennas: A Designer's Guide, R. Waterhouse, ISBN: 978-1-4757-3791-2
15. M. N. Jahromi, M. N. Jahromi, M. Rahman, "Switchable planar monopole antenna between ultra-wideband and narrow band behaviour," Progress Electromagn. Res. Letters 2018, 75, pp. 131–137.
16. X. L. Liu, et al., "A CPW-fed dual band-notched UWB antenna with a pair of bended dual-L-shape parasitic branches," Progress Electromagn. Res. 2013, 136, pp. 623–634.
17. R. Azim, M.-T. Islam, "Compact planar UWB antenna with band notch characteristics for WLAN and DSRC, "Progress Electromagn. Res. 2013, 133, pp. 391–406.
18. P. Lotfi, M. Azarmanesh, S. Soltani, "Rotatable dual band-notched UWB/triple-band WLAN reconfigurable antenna," IEEE Antennas Wirel. Propag. Lett. 2013, 12, pp. 104–107.
19. S. R. Emadian, et al., "Bandwidth enhancement of CPW-fed circle-like slot antenna with dual band-notched characteristic," IEEE Antennas Wirel. Propag. Lett. 2012, 11, pp. 543–546.
20. R. Fallahi, A. A. Kalteh, M. G. Roozbahani, "A novel UWB elliptical slot antenna with band-notched characteristics," Progress Electromagn. Res. 2008, 82, pp. 127–136.
21. J. Ding, Z. Lin, Z. Ying, S. A. He, "A compact ultra-wideband slot antenna with multiple notch frequency bands," Microw. Opt. Technol. Lett. 2007, 49, pp. 3056–3060.
22. S. Yadav, et al., "Design of dual band-notched lamp-shaped antenna with UWB characteristics," Int. J. Microw. Wirel. Technol. 2015, 9, pp. 395–402.
23. M. Rahman, et al., "Resonator based switching technique between ultra wide band (UWB) and single/dual continuously tunable-notch behaviors in UWB radar for wireless vital signs monitoring," Sensors 2018, 18, pp. 3330.
24. B. S. Yildirim, et al., "Integrated Bluetooth and UWB antenna," IEEE Antennas Wirel. Propag. Lett. 2009, 8, pp. 149–152.
25. R. Labade, et al., "A. Compact integrated Bluetooth UWB bandnotch antenna for personal wireless communication," Microw. Opt. Technol. Lett. 2016, 58, pp. 540–546.

26. W. Li, et al., “Planar antenna for 3G/Bluetooth/WiMAX and UWB applications with dual band notched characteristics,” IEEE Antennas Wirel. Propag. Lett. 2012, 11, pp. 61–64.
27. X. Kang, et al., “A band notched UWB printed half elliptical ring monopole antenna,” Progress Electromagn. Res. B 2013, 35, pp. 23–33.
28. T. Mandal, S. Das, S., “Design of a microstrip fed printed monopole antenna for Bluetooth and UWB applications with WLAN notch band characteristics,” Int. J. RF Microw. Comput. Aided Des. 2015, 25, pp. 66–74.
29. Z. Q. Li, et al., “Design and analysis of planar antenna with dual WLAN band-notched for integrated Bluetooth and UWB applications,” J. Electromagn. Waves Appl. 2010, 24, pp. 1817–1828.
30. S. K. Mishra, et al., “A compact dual-band fork-shaped monopole antenna for Bluetooth and UWB applications,” IEEE Antennas Wirel. Propag. Lett. 2011, 10, pp. 627–630.
31. K. Zhan, et al., “A miniature planar antenna for Bluetooth and UWB applications,” J. Electromagn. Waves Appl. 2010, 24, pp. 2299–2308.
32. M. Rahman, et al., “Compact UWB Band-Notched Antenna with Integrated Bluetooth for Personal Wireless Communication and UWB Applications,” Electronics 2019, 8(2), pp. 158.
33. M. Rahman, et al., ““Bandwidth enhancement and frequency scanning array antenna using novel UWB filter integration technique for OFDM UWB radar applications in wireless vital signs monitoring,” Sensors 2018, 18(9), pp. 3155.
34. A. Liu, Y. Lu, “A super-wide bandwidth low-profile monocone antenna with dielectric loading,” IEEE Transactions on Antennas and Propagation, Early Access, 29 March 2019.